Int. J. Anal. Appl. (2026), 24:266

International Journal of Analysis and Applications

A Spectral Galerkin Method with Hybrid Müntz–Jacobi Basis for Space–Time Fractional Advection–Diffusion Equations

Shahad Adil Taher*

Faculty of Computer Science and Mathematics, University of Kufa, Najaf, Iraq

**Corresponding author:* shahada.alkhafaji@uokufa.edu.iq

Abstract. For the numerical treatment of space-time fractional advection-diffusion equations, we designed a spectral Galerkin method. We construct the approximation space using a hybrid system of Müntz-Jacobi basis functions, combining the stability and orthogonality properties of Jacobi polynomials and the singularity-resolving capacity of Müntz-type monomials. The basis is reconstructed to satisfy homogeneous boundary conditions, thereby ensuring both consistency with the physical constraints and numerical stability. By including the dominant singular exponents of the exact solution into the approximation space, the suggested framework achieves exponential-type convergence with an accurate representation of endpoint singularities with high precision. We introduce the computational formulation, including the fractional integral and derivative of the new basis and the formulation of the Galerkin discretization.A series of numerical examples is provided, demonstrating the robustness and accuracy of the method for different fractional parameters, and agree with the theoretical error estimates. In general, the hybrid Müntz-Jacobi Galerkin framework achieves a flexible and powerful paradigm for fractional partial differential equations, with natural extensions to multi-term fractional operators, multi-dimensional models, and nonlinear systems.

1. Introduction

The concept of fractional calculus resulted from early discussions by L. Euler and G.W. Leibniz, who raised the question of whether the order of differentiation and integration must be restricted to integers.

What began as a theoretical curiosity has gradually extended into a rigorous mathematical discipline that generalises the principles of classical calculus to real or even complex orders.

This extension yields an effective framework for characterising dynamical systems in which 'long-range dependence, memory and 'nonlocal interactions' are intrinsic features.

Received: Jun. 6, 2026.

2020 *Mathematics Subject Classification.* 65M70.

Key words and phrases. fractional partial differential equations; spectral Galerkin method; numerical analysis; hybrid Müntz–Jacobi functions; exponential convergence; space–time fractional advection–diffusion equations; singularity-adapted basis; singularity index.

https://doi.org/10.28924/2291-8639-24-2026-266
ISSN: 2291-8639

During the nineteenth and early twentieth centuries, fractional operators received the interest of several leading mathematicians, including J.B.J. Fourier, P.S. Laplace, and N.H. Abel [7, 16, 21]. Modern formulations have proved a variety of operators, with the Riemann-Liouville and Caputo derivatives being among the most broadly used.

The Caputo formulation is appropriate for modelling physical systems; it aligns naturally with real-world problems as it accommodates classical initial conditions.

These advantages have led to fractional calculus being an essential tool in areas ranging from anomalous transport to bioengineering, viscoelasticity ,complex material modeling and control theory [12, 17, 25].

The field has developed substantially in recent decades, supported by the rise of international conferences, specialised journals, and a growing body of applications across the applied and natural sciences.

Due to the development of space-time fractional advection-diffusion equations, they have become powerful models for modelling anomalous transport phenomena in various fields, including contaminant transport in groundwater, viscoelastic flows, and plasma physics. Unlike fractional advection-diffusion equations incorporate fractional derivatives in both space and time and classical integer-order diffusion equations, capturing spatial heterogeneity effects and long-range temporal memory [13, 37].

The nonlocal nature of fractional derivatives significantly limits analytical solutions, usually restricting them to specific forms or simple boundary conditions

Hence, accurate and efficient numerical methods are essential for practical simulations. Classical numerical approaches, such as finite element, finite difference, and finite volume methods, face significant challenges when applied to fractional advection–diffusion equations, including high computational costs, loss of accuracy near singularities at domain boundaries, and dense matrices resulting from nonlocal operators [2, 15, 34].

Spectral Galerkin methods enable an effective alternative for fractional advection-diffusion equations attributable to their ability to project solutions onto global polynomial bases, attaining high-order or even spectral convergence for smooth solutions [18, 40]. Still, solutions of space-time fractional advection-diffusion problems often exhibit singular behaviours at the domain boundaries, such as $(1+x)^{\beta}$ near $x=-1$ or $(1-x)^{\gamma}$ near $x=1$, where the exponents β and γ are determined by the fractional orders and the structure of the operator. Classical polynomial bases, such as Chebyshev or Legendre polynomials, fail to approximate such singular solutions efficiently. motivating the development of singularity-aware spectral methods [11, 35, 36].

Time- and space-fractional differential equations have become essential for memory effects, modelling anomalous diffusion , nonlocal transport phenomena in science, engineering, and finance. Different numerical methods have been proposed to overcome challenges such as dense matrices, high computational cost, and boundary singularities. High-order schemes using Diethelm's

approach and finite elements have been developed for time-fractional PDEs with proven convergence [19], On the other hand, meshless approaches that use radial basis functions (RBFs) provide adaptable tools for stochastic advection-diffusion equations and handling multi-dimensional diffusion-wave phenomena [6, 22]. For spectral and operator-splitting methods and time-space fractional models, including improved L_1 schemes and modified homotopy perturbation methods, yield accurate and efficient solutions for problems such as the fractional Black–Scholes equation [5, 26]. These approaches collectively demonstrate the growing capability of high-order, meshless, and spectral techniques in capturing the complex dynamics of time- and space-fractional systems. To address these difficulties, recent research has emphasised enhancing spectral Galerkin schemes using specialised basis functions that embed endpoint singularities.

Müntz polynomials and Generalized Jacobi functions (GJFs) have been employed to incorporate known singular behaviours directly into the approximation space. significantly improving accuracy near singular points [10, 11, 24].

Despite this, conventional methods usually require a limited number of singularities, limiting flexibility for problems with multiple or compound singular behaviors. Hybrid approaches, like the hybrid Muntz-Jacobi method, provide a robust solution by combining multiple singularity indices while maintaining orthogonality and computational stability, making them highly suitable for fractional advection-diffusion equations with complex boundary-layer behaviors [41].

Also, we can see in [4,9,29] Bernstein polynomial-based spectral methods have observed notable effectiveness in handling fractional differential equations due to their natural compatibility with integral operators and strong approximation properties. When applied in a Galerkin approach, these bases allow accurate representation of space-time fractional advection-diffusion problems, including Riesz fractional advection-dispersion models and time-fractional reaction-diffusion systems [1, 33, 38].

Current research also includes operational matrices and collocation techniques for a reduction in computational complexity while preserving high accuracy near singularities [23, 28].

Overall, spectral Galerkin methods with singularity-aware and hybrid bases provide a flexible, efficient, and highly accurate framework for simulating fractional advection–diffusion equations, effectively capturing the nonlocal dynamics, singular behaviors, and multi-scale characteristics intrinsic to fractional advection–diffusion phenomena. In general, spectral Galerkin methods with singularity-aware and hybrid bases provide an efficient, flexible, and highly accurate framework to simulate fractional advection-diffusion equations. Successfully describe multi-scale characteristics intrinsic to fractional advection-diffusion phenomena, the singular behaviours, and nonlocal dynamics.

We develop a novel hybrid spectral Galerkin method using hybrid Müntz-Jacobi basis functions, which combine the algebraic flexibility of Müntz-type monomials with the stability and orthogonality properties of classical Jacobi polynomials. The hybrid basis is specifically designed

to address multiple algebraic singularities by appropriately selecting the exponents in the index set.

This represents a significant advancement over traditional approaches that typically handle at most a single singularity because this selection enables the method to accurately approximate solutions of fractional differential equations with more than one dominant singularity.

We also calculate the fractional integral and fractional differential of the new basis functions to enhance the applicability of the method.

This development yields a novel fractional basis that is well-suited for spectral approximations of fractional differential equations. In boundary value problems for fractional differential equations and in many practical applications , the chosen basis functions must vanish at the endpoints of the computational domain. A notable property of this formulation is that the chosen basis functions vanish at the domain boundaries. Thus, the approximate solution satisfies the homogeneous boundary conditions, avoiding the need for extra enforcement.

To achieve this, a compact modification of the original basis functions can be constructed, ensuring endpoint vanishing while preserving orthogonality and approximation capabilities.

The suggested method is then applied to solve space-time fractional advection-diffusion equations. These types of equations commonly involve both global integral terms and weakly singular kernels, presenting substantial challenges for classical numerical methods. Our approach handles these challenges effectively by capturing the inherent non-smoothness and the singular behaviour in the solution. Specifically, the method allows for highly accurate approximations even when singularities are near the domain boundaries or the solution exhibits sharp gradients.

Numerical examples verify the theoretical predictions and demonstrate that the developed method significantly outperforms classical spectral schemes, especially in cases where the solution exhibits multiple singularities or is non-smooth. The results show that the hybrid basis not only reduces computational errors compared to traditional polynomial-based methods but also improves convergence rates.

2. Preliminaries

In this section, we present the main preliminaries of fractional calculus. The discussion includes the left- and right-sided forms of fractional integrals and derivatives defined in the Riemann–Liouville and Caputo sense, along with their essential properties. We also review the basic features and relations of Jacobi and Müntz–Legendre polynomials that will be used in the subsequent analysis.

2.1. **Definitions.**

Definition 2.1 (Riemann–Liouville and Caputo fractional operators)**.** *Let $v(x)$ be a sufficiently smooth real-valued function on $[a,b]$, and let $\alpha > 0$. We define (see [17, 25])*

(i) Riemann–Liouville fractional integrals:

$$ {}_aI_x^\alpha v(x) := \frac{1}{\Gamma(\alpha)} \int_a^x (x-s)^{\alpha-1} v(s)\, ds, \qquad \textit{(left-sided)}, \tag{2.1} $$

$$ {}_xI_b^\alpha v(x) := \frac{1}{\Gamma(\alpha)} \int_x^b (s-x)^{\alpha-1} v(s)\, ds, \qquad \textit{(right-sided)}. \tag{2.2} $$

(ii) Caputo fractional derivatives: *Let $\alpha \in (m-1, m)$ with $m \in \mathbb{N}$. Then*

$$ {}_a^{\mathrm{C}}D_x^\alpha v(x) := {}_aI_x^{m-\alpha}\left(\frac{d^m v(x)}{dx^m}\right), \qquad \textit{(left-sided)}, \tag{2.3} $$

$$ {}_x^{\mathrm{C}}D_b^\alpha v(x) := (-1)^m\, {}_xI_b^{m-\alpha}\left(\frac{d^m v(x)}{dx^m}\right), \qquad \textit{(right-sided)}. \tag{2.4} $$

In the following, some fundamental properties and interrelationships between fractional integrals and derivatives are presented and discussed, highlighting their role in fractional calculus theory and applications.

Theorem 2.1 (Affine transformation)**.** *Let $x = \frac{b-a}{2}\tau + \frac{b+a}{2}$ map $[a, b]$ onto $[-1, 1]$. Then the fractional operators satisfy*

$$ {}_aI_x^\alpha v(x) = \left(\frac{b-a}{2}\right)^\alpha {}_{-1}I_\tau^\alpha v(\tau; a, b), \qquad {}_a^{\mathrm{C}}D_x^\alpha v(x) = \left(\frac{2}{b-a}\right)^\alpha {}_{-1}^{\mathrm{C}}D_\tau^\alpha v(\tau; a, b), \tag{2.5} $$

$$ {}_xI_b^\alpha v(x) = \left(\frac{b-a}{2}\right)^\alpha {}_\tau I_1^\alpha v(\tau; a, b), \qquad {}_x^{\mathrm{C}}D_b^\alpha v(x) = \left(\frac{2}{b-a}\right)^\alpha {}_\tau^{\mathrm{C}}D_1^\alpha v(\tau; a, b). \tag{2.6} $$

The Riemann–Liouville fractional derivative, in terms of the Caputo fractional derivative, can be expressed as follows:

Lemma 2.1. *Let $\alpha \in (m-1, m)$, $m \in \mathbb{N}$. For sufficiently smooth $v(x)$ we have*

$$ {}_aD_x^\alpha v(x) = {}_a^{\mathrm{C}}D_x^\alpha v(x) + \sum_{k=0}^{m-1} \frac{v^{(k)}(a)}{\Gamma(k-\alpha+1)} (x-a)^{k-\alpha}, \tag{2.7} $$

$$ {}_xD_b^\alpha v(x) = {}_x^{\mathrm{C}}D_b^\alpha v(x) + \sum_{k=0}^{m-1} \frac{(-1)^k v^{(k)}(b)}{\Gamma(k-\alpha+1)} (b-x)^{k-\alpha}. \tag{2.8} $$

In particular, if $v^{(k)}(a) = 0$ (resp. $v^{(k)}(b) = 0$) for $k = 0, \ldots, m-1$, the left-sided (resp. right-sided) Riemann–Liouville and Caputo derivatives coincide.

Theorem 2.2 (Composition rules)**.** *Let $\alpha \geq \beta > 0$. Then*

$$ {}_aI_x^\beta \left({}_a^{\mathrm{C}}D_x^\alpha v(x)\right) = {}_a^{\mathrm{C}}D_x^{\alpha-\beta} v(x) - \sum_{k=\lceil \alpha-\beta \rceil}^{\lceil \alpha \rceil - 1} \frac{v^{(k)}(a)}{\Gamma(k+\beta-\alpha+1)} (x-a)^{k+\beta-\alpha}, \tag{2.9} $$

$$ {}_xI_b^\beta \left({}_x^{\mathrm{C}}D_b^\alpha v(x)\right) = {}_x^{\mathrm{C}}D_b^{\alpha-\beta} v(x) - \sum_{k=\lceil \alpha-\beta \rceil}^{\lceil \alpha \rceil - 1} \frac{(-1)^k v^{(k)}(b)}{\Gamma(k+\beta-\alpha+1)} (b-x)^{k+\beta-\alpha}. \tag{2.10} $$

Theorem 2.3 (Action on power functions). *Let $\beta > -1$ and $\alpha > 0$. Then*

$$ {}_aI_x^\alpha (x-a)^\beta = \frac{\Gamma(\beta+1)}{\Gamma(\beta+\alpha+1)}(x-a)^{\beta+\alpha}, \qquad {}_xI_b^\alpha (b-x)^\beta = \frac{\Gamma(\beta+1)}{\Gamma(\beta+\alpha+1)}(b-x)^{\beta+\alpha}. \tag{2.11} $$

Moreover, for $\beta > m-1$, $m-1 < \alpha < m$,

$$ {}^{\mathrm{C}}_aD_x^\alpha (x-a)^\beta = \frac{\Gamma(\beta+1)}{\Gamma(\beta-\alpha+1)}(x-a)^{\beta-\alpha}, \qquad {}^{\mathrm{C}}_xD_b^\alpha (b-x)^\beta = \frac{(-1)^m\Gamma(\beta+1)}{\Gamma(\beta-\alpha+1)}(b-x)^{\beta-\alpha}. \tag{2.12} $$

If $\beta \in \mathbb{N}_0$ and $\beta \le m-1$, the Caputo derivatives vanish.

The following result [11] plays fundamental roles in the analysis of fractional calculus. For all $0 < \alpha < 2$ and $\alpha \neq 1$, we have

$$ ({}_{-1}D_x^\alpha u, v)_\Lambda = ({}_{-1}D_x^{\frac{\alpha}{2}} u, {}_x D_1^{\frac{\alpha}{2}} v)_\Omega, $$

where $\Omega = (-1, 1)$.

Remark 2.1. *The right-sided operators can be interpreted as the left-sided operators applied to a function reflected with respect to $x \mapsto b - a - x$. This duality is often useful in the derivation of symmetric numerical schemes.*

2.2. **Jacobi Polynomials and Two-Sided Generalized Jacobi Functions (GJFs).** Jacobi polynomials form a classical class of orthogonal polynomials that possess rich structural characteristics and are widely used in spectral discretizations for differential and fractional differential equations (see [11, 31]). For real parameters $\alpha, \beta > -1$, the family of Jacobi polynomials $\{P_n^{(\alpha,\beta)}(x)\}_{n=0}^\infty$ is orthogonal on the interval $[-1, 1]$ with respect to the weight function

$$ \omega^{(\alpha,\beta)}(x) = (1-x)^\alpha (1+x)^\beta, $$

that is,

$$ \int_{-1}^{1} P_n^{(\alpha,\beta)}(x)\, P_m^{(\alpha,\beta)}(x)\, \omega^{(\alpha,\beta)}(x)\, dx = \gamma_n^{(\alpha,\beta)}\, \delta_{nm}, $$

where δ_{nm} denotes the Kronecker delta and

$$ \gamma_n^{(\alpha,\beta)} = \frac{2^{\alpha+\beta+1}\,\Gamma(n+\alpha+1)\,\Gamma(n+\beta+1)}{(2n+\alpha+\beta+1)\,n!\,\Gamma(n+\alpha+\beta+1)}. $$

These polynomials can also be represented using the hypergeometric function

$$ \begin{aligned} P_n^{(\alpha,\beta)}(x) &= \frac{(\beta+1)_n}{n!}\, {}_2F_1\Big(-n,\, n+\alpha+\beta+1;\, \beta+1;\, \frac{1+x}{2}\Big) \\ &= \frac{(\alpha+1)_n}{n!}\, {}_2F_1\Big(-n,\, n+\alpha+\beta+1;\, \alpha+1;\, \frac{1-x}{2}\Big), \end{aligned} $$

or equivalently through the explicit expansion

$$ P_n^{(\alpha,\beta)}(x) = \sum_{k=0}^{n} {}^1d_{k,n}^{(\alpha,\beta)}\, (1+x)^k = \sum_{k=0}^{n} {}^2d_{k,n}^{(\alpha,\beta)}\, (1-x)^k, $$

with the coefficients given by

$$ {}^{1}d_{k,n}^{(\alpha,\beta)} = \frac{(-1)^k\,\Gamma(n+\beta+1)\,\Gamma(n+k+\alpha+\beta+1)}{2^k\,\Gamma(n+\alpha+\beta+1)\,k!\,(n-k)!\,\Gamma(k+\beta+1)}, $$

and

$$ {}^{2}d_{k,n}^{(\alpha,\beta)} = \frac{(-1)^k\,\Gamma(n+\alpha+1)\,\Gamma(n+k+\alpha+\beta+1)}{2^k\,\Gamma(n+\alpha+\beta+1)\,k!\,(n-k)!\,\Gamma(k+\alpha+1)}. $$

To effectively approximate solutions of fractional differential equations exhibiting endpoint singularities, one often employs *generalized Jacobi functions* (GJFs), sometimes called *polyfractonomials*. For $\alpha \in \mathbb{R}$ and $\beta > -1$, the left- and right-sided GJFs are defined by

$$ {}^{-}J_n^{(\alpha,\beta)}(x) := (1+x)^{\beta}\,P_n^{(\alpha,\beta)}(x), \qquad {}^{+}J_n^{(\alpha,\beta)}(x) := (1-x)^{\alpha}\,P_n^{(\alpha,\beta)}(x). $$

These functions preserve orthogonality under modified weight functions and are well-suited for representing endpoint singularities.

Fractional integrals and derivatives. Let $\rho, s > 0$ and $n \in \mathbb{N}_0$. For $\alpha \in \mathbb{R}$ and $\beta > -1$, the *left-sided* Riemann–Liouville fractional integral of order ρ acts on ${}^{-}J_n^{(\alpha,\beta)}$ as

$$ {}_{-1}I_x^{\rho}\Big[(1+x)^{\beta}P_n^{(\alpha,\beta)}(x)\Big] = \frac{\Gamma(n+\beta+1)}{\Gamma(n+\beta+\rho+1)}\,(1+x)^{\beta+\rho}\,P_n^{(\alpha-\rho,\beta+\rho)}(x), \tag{2.13} $$

while the corresponding *right-sided* integral satisfies

$$ {}_{x}I_1^{\rho}\Big[(1-x)^{\alpha}P_n^{(\alpha,\beta)}(x)\Big] = \frac{\Gamma(n+\alpha+1)}{\Gamma(n+\alpha+\rho+1)}\,(1-x)^{\alpha+\rho}\,P_n^{(\alpha+\rho,\beta-\rho)}(x). \tag{2.14} $$

Similarly, the *left-sided* Riemann–Liouville fractional derivative of order s yields

$$ {}_{-1}D_x^{s}\Big[(1+x)^{\beta+s}P_n^{(\alpha-s,\beta+s)}(x)\Big] = \frac{\Gamma(n+\beta+s+1)}{\Gamma(n+\beta+1)}\,(1+x)^{\beta}\,P_n^{(\alpha,\beta)}(x), \tag{2.15} $$

and the *right-sided* counterpart is given by

$$ {}_{x}D_1^{s}\Big[(1-x)^{\alpha+s}P_n^{(\alpha+s,\beta-s)}(x)\Big] = \frac{\Gamma(n+\alpha+s+1)}{\Gamma(n+\alpha+1)}\,(1-x)^{\alpha}\,P_n^{(\alpha,\beta)}(x). \tag{2.16} $$

Also, for $s \in \mathbb{R}^{+}$, $\alpha \in \mathbb{R}$, and $\beta > s-1$.

$$ {}_{-1}D_x^{s}\,{}^{-}J_n^{(\alpha,\beta)}(x) = \frac{\Gamma(n+\beta+1)}{\Gamma(n+\beta-s+1)}\,{}^{-}J_n^{(\alpha+s,\beta-s)}(x), \tag{2.17} $$

and for $s \in \mathbb{R}^{+}$, $\beta \in \mathbb{R}$, and $\alpha > s-1$.

$$ {}_{x}D_1^{s}\,{}^{+}J_n^{(\alpha,\beta)}(x) = \frac{\Gamma(n+\alpha+1)}{\Gamma(n+\alpha-s+1)}\,{}^{+}J_n^{(\alpha-s,\beta+s)}(x). \tag{2.18} $$

In particular, for the special case $\alpha = \beta = 0$, the above formulas reduce to identities involving Legendre polynomials $P_n(x)$:

$$ {}_{-1}I_x^{\rho}\left[P_n(x)\right] = \frac{n!}{\Gamma(n+\rho+1)}\,(1+x)^{\rho}\,P_n^{(-\rho,\rho)}(x), $$

$$ {}_{x}I_1^{\rho}\left[P_n(x)\right] = \frac{n!}{\Gamma(n+\rho+1)}\,(1-x)^{\rho}\,P_n^{(\rho,-\rho)}(x). $$

Analogous simplifications hold for the fractional derivatives. These two-sided relations highlight the parameter-shifting structure induced by fractional operators on Jacobi polynomial-based functions.

2.3. **Generalized Müntz Systems on the Interval** $[-1,1]$**.** Let $\Lambda = \{\lambda_k\}_{k=0}^{\infty}$ denote a strictly increasing sequence of real numbers satisfying

$$\lambda_0 < \lambda_1 < \lambda_2 < \cdots, \qquad \lambda_k > -\frac{1}{2}, \quad k \geq 0,$$

(see, e.g., [14, 20, 24, 32]). The classical Müntz system on $[0,1]$ consists of monomials $\{x^{\lambda_k}\}_{k=0}^{\infty}$. By the affine transformations

$$\xi_1 := \frac{1+x}{2}, \quad \xi_2 := \frac{1-x}{2} \quad x \in [-1,1],$$

we define two classes of the *transformed Müntz systems* over the symmetric interval $[-1,1]$ as

$${}^{i}\mathcal{T}_n(\Lambda) := \operatorname{span}\left\{\xi_i^{\lambda_0}, \xi_i^{\lambda_1}, \ldots, \xi_i^{\lambda_n}\right\}; \quad i = 1,2,$$

with infinite-dimensional subspaces

$${}^{i}\mathcal{T}(\Lambda) = \bigcup_{n=0}^{\infty} {}^{i}\mathcal{T}_n(\Lambda), \quad i = 1,2.$$

Theorem 2.4. *The set of Müntz-type polynomials*

$$\sum_{k=0}^{n} a_k (1 \pm x)^{\lambda_k}$$

is dense in the Hilbert space $L^2([-1,1])$ *if and only if*

$$\sum_{k=1}^{\infty} \frac{1}{\lambda_k} = +\infty. \tag{2.19}$$

Generalized Müntz–Legendre polynomials. Orthogonal bases of $\mathcal{T}_n(\Lambda)$ can be constructed via contour integrals:

$$\mathcal{L}_n(x;\Lambda) := \frac{1}{2\pi i} \int_{\Gamma} \left[\prod_{k=0}^{n-1} \frac{t+\lambda_k+1}{t-\lambda_k}\right] \frac{\left(\frac{1\pm x}{2}\right)^t}{t-\lambda_n}\, dt,$$

where Γ is a closed contour encircling $t = \lambda_0, \ldots, \lambda_n$. These polynomials admit the expansion

$${}^{-}\mathcal{L}_n(x;\Lambda) = \sum_{k=0}^{n} a_{k,n} (1+x)^{\lambda_k}, \quad {}^{+}\mathcal{L}_n(x;\Lambda) = \sum_{k=0}^{n} a_{k,n} (1-x)^{\lambda_k}, \tag{2.20}$$

$$a_{k,n} = \frac{\prod_{j=0}^{n-1} (\lambda_k + \lambda_j + 1)}{2^{\lambda_k} \prod_{\substack{j=0 \\ j \neq k}}^{n-1} (\lambda_k - \lambda_j)}.$$

It is easy to prove that ${}^{-}\mathcal{L}_n(1;\Lambda) = {}^{+}\mathcal{L}_n(-1;\Lambda) = 1$ and

$${}^{-}\mathcal{L}_n(-1;\Lambda) = {}^{+}\mathcal{L}_n(1;\Lambda) = \begin{cases} 0; & \lambda_0 > 0, \\ a_{0,n}; & \lambda_0 = 0. \end{cases}$$

They are mutually orthogonal in $L^2([-1,1])$ with respect to $\omega(x)=1$:

$$\int_{-1}^{1} {}^{\pm}\mathcal{L}_n(x;\Lambda)\,{}^{\pm}\mathcal{L}_m(x;\Lambda)\,dx = \delta_{nm}\frac{2}{2\lambda_n+1}.$$

3. Definition of Hybrid Müntz–Jacobi Functions

Classical orthogonal polynomial bases are not well-suited for approximating functions with singular behaviour near the boundaries of the interval, particularly at the endpoints. The main reason is that the generalized polynomial bases, namely GJFs, are typically constructed to accommodate only a single singular index, which makes them insufficient for functions that display more singular index terms. While generalized Jacobi functions $J_n^{(\alpha,\beta)}(x)$ can accommodate a single singularity through their parameters α and β, they fail to capture functions with multiple singularities at both boundaries.

To address this, we introduce a novel hybrid approach that combines the strengths of generalized Jacobi functions with Müntz systems. This hybrid method allows for the efficient approximation of functions with multiple singularities at least three simultaneously, enabling a more accurate representation of functions with complex behaviors. The developed basis functions resolve singularities at multiple endpoints and maintain high accuracy in approximating fractional models and other problems with singular features.

3.1. **Hybrid Basis Construction.** To accurately capture endpoint behavior, we define a family of fractional indices that act as parameters governing the singularities of the constructed basis functions.. Let the indices be such that:

$$\beta_1 < \beta_2 < \beta_3,$$

and define the generalized Müntz-type index set as:

$$\Lambda = \{0, \beta_1, \beta_2, \beta_3, 1+\beta_1, 1+\beta_2, 1+\beta_3, \ldots\}.$$

The defined indices are crucial for the hybrid construction, since they govern the singular behavior at both boundaries, $x=-1$ and $x=1$. Accordingly, the basis functions $\mathcal{L}_n^{(\beta_1,\beta_2,\beta_3)}(x)$ are represented in terms of generalized Jacobi polynomials, and will hereafter be denoted by $\mathcal{L}_n^{(\beta_i)}(x)$. For this goal, we define:

$${}^{-}\mathcal{L}_n^{(\beta_i)}(x) = a_{0,n} + \sum_{i=1}^{3}\sum_{k=0}^{n_i} a_{3k+i,n}(1+x)^{k+\beta_i},$$

equivalently, we have:

$${}^{-}\mathcal{L}_n^{(\beta_i)}(x) = a_{0,n} + \sum_{i=1}^{3}(1+x)^{\beta_i}\,{}^{-}\varphi_{n_i}(x),$$

and similarly for the positive side:

$${}^{+}\mathcal{L}_n^{(\beta_i)}(x) = a_{0,n} + \sum_{1}^{3}\sum_{k=0}^{n_i} a_{3k+i,n}(1-x)^{k+\beta_i},$$

which simplifies to:

$$^{+}\mathcal{L}_n^{(\beta_i)}(x) = a_{0,n} + \sum_{i=1}^{3}(1-x)^{\beta_i}\,{}^{+}\varphi_{n_i}(x).$$

Here, the index n_i is given by:

$$n_i = \left\lfloor \frac{n-i}{3} \right\rfloor, \quad i = 1, 2, 3.$$

Multiple singularities are represented by including, for each index β_i, the factors $(1+x)^{\beta_i}$ and $(1-x)^{\beta_i}$.

3.2. **Recursive Computation of Coefficients.** The coefficients $a_{k,n}$ exhibit rapid growth with respect to n, which may compromise numerical stability. To address this difficulty, we adopt a recursive algorithm for generating the Jacobi expansion coefficients. In this framework, each $\varphi_{n_i}(x)$ is expanded through generalized Jacobi polynomials, ensuring stable and efficient evaluation. The monomial representation of $\varphi_{n_i}(x)$ is then written as:

$$^{\pm}\varphi_{n_i}(x) = \sum_{k=0}^{n_i} a_{3k+i,n}(1 \pm x)^k.$$

We now rewrite these functions using Jacobi polynomials with parameters $(-\beta_i, \beta_i)$ and $(\beta_i, -\beta_i)$, respectively, in the form:

$$^{-}\varphi_{n_i}(x) = \sum_{j=0}^{n_i} {}^{1}c_{j,n_i} P_j^{(-\beta_i,\beta_i)}(x) = \sum_{j=0}^{n_i}\sum_{r=0}^{j} {}^{1}c_{j,n_i}\,{}^{1}d_{r,j}^{(-\beta_i,\beta_i)}(1+x)^r,$$

and similarly for the positive side:

$$^{+}\varphi_{n_i}(x) = \sum_{j=0}^{n_i} {}^{2}c_{j,n_i} P_j^{(\beta_i,-\beta_i)}(x) = \sum_{j=0}^{n_i}\sum_{r=0}^{j} {}^{2}c_{j,n_i}\,{}^{2}d_{r,j}^{(\beta_i,-\beta_i)}(1-x)^r.$$

Equating the coefficients associated with equal powers of $(1+x)^k$ in both representations, we obtain the following lower triangular system:

$$a_{3k+i,n} = \sum_{j=k}^{n_i} {}^{1}c_{j,n_i}\,{}^{1}d_{k,j}^{(-\beta_i,\beta_i)}, \quad k = 0, 1, \ldots, n_i.$$

For computing ${}^{1}c_{j,n_i}$ and ${}^{2}c_{j,n_i}$, there are some robust strategies, such as solving the lower-triangular system directly or using a different orthogonalization process, that could be employed if instability were to arise. Here, we use a recursive back-substitution algorithm for computing the Jacobi expansion coeffcients. Because the coefficient matrix has a lower triangular structure, the expansion coefficients ${}^{1}c_{j,n_i}$ are determined recursively. As a first step, for $j = 0$ one finds:

$${}^{1}c_{0,n_i} = \frac{a_{i,n}}{{}^{1}d_{0,0}^{(-\beta_i,\beta_i)}},$$

and for $j = 1, 2, \ldots, n_i$:

$$ {}^{1}c_{j,n_i} = \frac{1}{{}^{1}d_{j,j}^{(-\beta_i,\beta_i)}} \left(a_{3j+i,n} - \sum_{k=0}^{j-1} {}^{1}c_{k,n_i} \, {}^{1}d_{3j+i,k}^{(-\beta_i,\beta_i)} \right). $$

By construction, the recursive algorithm provides a reliable and systematic approach for computing the Jacobi expansion coefficients linked to the hybrid Müntz–Jacobi basis. A comparable recursion applies to the coefficients ${}^{2}c_{j,n_i}$ corresponding to the positive side.

There are some robust strategies, such as solving the lower-triangular system directly or using a different orthogonalization process, that could be employed if instability were to arise. Here, we use a recursive back-substitution algorithm for computing the Jacobi expansion coeffcients

3.3. **Hybrid Expansion and Applications in Fractional Calculus.** The hybrid formulation admits the following representation in terms of generalized Jacobi polynomials:

$$ {}^{-}\mathcal{L}_n^{(\beta_i)}(x) = a_{0,n} + \sum_{i=1}^{3} \sum_{j=0}^{n_1} {}^{1}c_{j,n_i} \, {}^{-}J_j^{(-\beta_i,\beta_i)}(x), $$

and similarly for the right-side:

$$ {}^{+}\mathcal{L}_n^{(\beta_i)}(x) = a_{0,n} + \sum_{i=1}^{3} \sum_{j=0}^{n_i} {}^{2}c_{j,n_i} \, {}^{+}J_j^{(\beta_i,-\beta_i)}(x). $$

Beyond resolving multiple singular behaviors, the hybrid construction extends to operations of fractional calculus, in particular to fractional integrals and derivatives. In the case of fractional integrals, the formulas take the form:

$$ {}_{-1}I_x^{\alpha} \, {}^{-}\mathcal{L}_n^{(\beta_i)}(x) = \frac{a_{0,n}}{\Gamma(\alpha+1)}(1+x)^{\alpha} + \sum_{i=1}^{3} \sum_{j=0}^{n_i} c_{j,n_i} \frac{\Gamma(j+\beta_i+1)}{\Gamma(j+\beta_i+\alpha+1)} \, {}^{-}J_j^{(-\beta_i-\alpha,\beta_i+\alpha)}(x), $$

and similarly for the right-side fractional integral:

$$ {}_{x}I_1^{\alpha} \, {}^{+}\mathcal{L}_n^{(\beta_i)}(x) = \frac{a_{0,n}}{\Gamma(\alpha+1)}(1-x)^{\alpha} + \sum_{i=1}^{3} \sum_{j=0}^{n_i} c_{j,n_i} \frac{\Gamma(j+\beta_i+1)}{\Gamma(j+\beta_i+\alpha+1)} \, {}^{+}J_j^{(\beta_i+\alpha,-\beta_i-\alpha)}(x). $$

Similarly, the fractional derivatives are expressed as:

$$ {}_{-1}^{C}D_x^{\alpha} \, {}^{-}\mathcal{L}_n^{(\beta_i)}(x) = \sum_{i=1}^{3} \sum_{j=0}^{n_i} c_{j,n_i} \frac{\Gamma(j+\beta_i+1)}{\Gamma(j+\beta_i-\alpha+1)} \, {}^{-}J_j^{(\alpha-\beta_i,\beta_i-\alpha)}(x), $$

and for the right-side fractional derivative:

$$ {}_{x}^{C}D_1^{\alpha} \, {}^{+}\mathcal{L}_n^{(\beta_i)}(x) = \sum_{i=1}^{3} \sum_{j=0}^{n_i} c_{j,n_i} \frac{\Gamma(j+\beta_i+1)}{\Gamma(j+\beta_i-\alpha+1)} \, {}^{+}J_j^{(-\alpha+\beta_i,-\beta_i+\alpha)}(x). $$

For left-sided Riemann–Liouville fractional derivative on the interval $[-1, 1]$, one obtains

$$ {}_{-1}D_x^{\alpha} \, {}^{-}\mathcal{L}_n^{(\beta_i)}(x) = \frac{a_{0,n}}{\Gamma(1-\alpha)}(1+x)^{-\alpha} + \sum_{i=1}^{3} \sum_{j=0}^{n_i} c_{j,n_i} \frac{\Gamma(j+\beta_i+1)}{\Gamma(j+\beta_i-\alpha+1)} \, {}^{-}J_j^{(\alpha-\beta_i,\beta_i-\alpha)}(x). \tag{3.1} $$

Similarly, for the right-sided fractional derivative, one has

$$ {}_xD_1^{\alpha}\,{}^{+}\mathcal{L}_n^{(\beta_i)}(x) = \frac{a_{0,n}}{\Gamma(1-\alpha)}(1-x)^{-\alpha} + \sum_{i=1}^{3}\sum_{j=0}^{n_i} c_{j,n_i}\,\frac{\Gamma(j+\beta_i+1)}{\Gamma(j+\beta_i-\alpha+1)}\,{}^{+}J_j^{(-\alpha+\beta_i,-\beta_i+\alpha)}(x). \tag{3.2} $$

In many practical applications, particularly those involving boundary value problems for fractional differential equations, it is desirable that the chosen basis functions vanish at the domain endpoints. This ensures that the numerical approximation automatically satisfies homogeneous boundary conditions.

To this end, one may construct a compact modification of the original basis functions as follows. For the left-sided basis we define

$$ {}^{-}\phi_n^{(\beta_i)}(x) = {}^{-}\mathcal{L}_n^{(\beta_i)}(x) - \frac{a_{0,n+2}-a_{0,n}}{a_{0,n+2}-a_{0,n+1}}\,{}^{-}\mathcal{L}_{n+1}^{(\beta_i)}(x) + \frac{a_{0,n+1}-a_{0,n}}{a_{0,n+2}-a_{0,n+1}}\,{}^{-}\mathcal{L}_{n+2}^{(\beta_i)}(x), \tag{3.3} $$

and for the right-sided basis we analogously set

$$ {}^{+}\phi_n^{(\beta_i)}(x) = {}^{+}\mathcal{L}_n^{(\beta_i)}(x) - \frac{a_{0,n+2}-a_{0,n}}{a_{0,n+2}-a_{0,n+1}}\,{}^{+}\mathcal{L}_{n+1}^{(\beta_i)}(x) + \frac{a_{0,n+1}-a_{0,n}}{a_{0,n+2}-a_{0,n+1}}\,{}^{+}\mathcal{L}_{n+2}^{(\beta_i)}(x), \tag{3.4} $$

By construction, these modified basis functions satisfy the homogeneous boundary conditions

$$ {}^{-}\phi_n^{(\beta_i)}(-1) = {}^{+}\phi_n^{(\beta_i)}(-1) = {}^{-}\phi_n^{(\beta_i)}(1) = {}^{+}\phi_n^{(\beta_i)}(1) = 0. $$

This formulation not only paves the way for solving complex fractional differential equations that involve such functions but also provides a more stable and efficient approach to approximating functions with multiple singularities.

4. Spectral Galerkin Approach on the Finite Interval

In this section, we consider the nonlinear space-time fractional advection-diffusion problem as:

$$ {}_{-1}^{C}D_t^{\gamma}u(x,t) + k_1\,u_t(x,t) + k_2\,u_x(x,t) + k_3\,{}_{-1}D_x^{\alpha}u(x,t) + \mathcal{N}(u(x,t),t) = 0, \qquad (x,t)\in\Omega^2, \tag{4.1} $$

where $0<\gamma<1$, $0<\alpha<2$ with $\alpha\neq 1$.
$\mathcal{N}(u,t)$: represents the nonlinear component of the model.

The formulation is complemented with the initial and boundary conditions

$$ u(x,-1) = 0, \quad x\in\Omega, \qquad u(-1,t) = u(1,t) = 0, \quad t\in\Omega. $$

More broadly, with non-homogeneous initial conditions, we can define the problem on a rectangle $(x,t)\in(a,b)\times(c,d)$.

$$ u(x,a) = g(x), \qquad x\in(a,b). $$

and with applying Theorem 2.1 and introducing the transformation

$$ \tilde{u}(x,t) := u(x,t) - g(x), $$

With homogeneous initial conditions, the problem can be reformulated on the normalized square domain $(x,t)\in(-1,1)^2$, which is often more suitable for theoretical analysis and numerical treatment.

Equation (4.1) includes several important limiting cases. For instance, if $\alpha = 2$, the operator ${}_{-1}D_t^{\alpha}$ reduces to the classical second-order derivative, and the model includes a standard diffusion term in time. If $\gamma = 1$, the Caputo derivative becomes the ordinary first-order derivative, recovering the structure of the classical advection-diffusion equation. Setting $k_2 = 0$ leads to a purely time-fractional diffusion model, while eliminating k_1 and k_3 reduces the formulation to a space-fractional advection equation. The problem is linear when the nonlinear part vanishes, i.e., $\mathcal{N}(u,t) = k_4 u(x,t) - f(x,t)$; otherwise, the nonlinear term plays a crucial role in capturing complex dynamics such as anomalous reactions, nonlinear transport, or memory-dependent feedbacks. This flexibility ensures the model (4.1) a powerful framework for describing a wide range of anomalous diffusion and transport phenomena.

The corresponding space-time Galerkin spectral method for (4.2) seeks $u \in \mathbb{V}_{M,N}$ such that for all $v \in \mathbb{V}_{M,N}$,

$$\mathcal{A}(u,v) := ({}_{-1}^{C}D_t^{\gamma} u, v) + k_1 (u_t, v) + k_2 (u_x, v) + k_3 ({}_{-1}D_x^{\alpha} u, v) + (\mathcal{N}(u,\cdot), v) = 0. \tag{4.2}$$

Here, $(\cdot,\cdot)$ denotes the $L^2(-1,1)$ inner product in the relevant variable, and the double inner product $\langle \cdot,\cdot \rangle$ is used on $(-1,1)^2$ when needed. The space $\mathbb{V}_{M,N}$ is defined as:

$$\mathbb{V}_{M,N} := \mathcal{F}_M^{(\beta_i)} \otimes \mathcal{F}_N^{(\beta_i')},$$

where

$$\mathcal{F}_M^{(\beta_i)} = \operatorname{span}\left\{ {}^{-}\phi_m^{(\beta_i)}(x) : 0 \le m \le M \right\},$$

and

$$\mathcal{F}_N^{(\beta_i')} = \operatorname{span}\left\{ {}^{-}\phi_n^{(\beta_i')}(t) : 0 \le n \le N \right\}.$$

We approximate the solution by

$$u_{M,N}(x,t) = \sum_{m=0}^{M} \sum_{n=0}^{N} u_{mn}\, {}^{-}\phi_m^{(\beta_i)}(x)\, {}^{-}\phi_n^{(\beta_i')}(t) = \Psi_x(x)\, \boldsymbol{\mathcal{U}}\, \Psi_t(t)^T,$$

where $\boldsymbol{\mathcal{U}} = (u_{mn}) \in \mathbb{R}^{(M+1)\times(N+1)}$, and

$$\Psi_x(x) = \left({}^{-}\phi_0^{(\beta_i)}(x), \ldots, {}^{-}\phi_M^{(\beta_i)}(x) \right), \quad \Psi_t(t) = \left({}^{-}\phi_0^{(\beta_i')}(t), \ldots, {}^{-}\phi_N^{(\beta_i')}(t) \right).$$

The triples $\beta_i = (\beta_1, \beta_2, \beta_3)$ and $\beta_i' = (\beta_1', \beta_2', \beta_3')$ encode the endpoint singular indexes of the unknowns in x and t, respectively. In practice, these exponents are determined via asymptotic analysis [35,36], which reveals the local singular behavior of the solution. As an illustration, close to the spatial boundary, the solution exhibits the following behavior:

$$u(x,t) \sim \sum_{i=1}^{3} c_i(t)\, (1+x)^{\beta_i}, \quad \text{as} \quad x \to -1^{+},$$

and near the temporal boundary, the behavior is given by

$$u(x,t) \sim \sum_{i=1}^{3} c_i'(x)\, (1+t)^{\beta_i'}, \quad \text{as} \quad t \to -1^{+}.$$

The sets of indices $\{\beta_i\}$ and $\{\beta_i'\}$ are determined from the asymptotic behavior and projected onto the admissible family of fractional basis functions by rounding to the nearest elements. Such a construction allows the trial space to reproduce the algebraic singularities at the endpoints and leads to almost optimal *hp*-convergence for fractional diffusion–advection equations with boundary layers.

Using test functions $v(x,t) = {}^{-}\phi_j^{(\beta_i)}(x)\,{}^{-}\phi_k^{(\beta_i')}(t)$, where $0 \le j \le M$ and $0 \le k \le N$, the discrete equations read

$$\begin{aligned}\sum_{m=0}^{M}\sum_{n=0}^{N} u_{mn}\Bigg[&\left({}^{-}\phi_m^{(\beta_i)}, {}^{-}\phi_j^{(\beta_i)}\right)_x \left({}_{-1}^{C}D_t^{\gamma}\,{}^{-}\phi_n^{(\beta_i')}, {}^{-}\phi_k^{(\beta_i')}\right)_t \\ &+ k_1\left({}^{-}\phi_m^{(\beta_i)}, {}^{-}\phi_j^{(\beta_i)}\right)_x \left(\partial_t\,{}^{-}\phi_n^{(\beta_i')}, {}^{-}\phi_k^{(\beta_i')}\right)_t \\ &+ k_2\left(\partial_x\,{}^{-}\phi_m^{(\beta_i)}, {}^{-}\phi_j^{(\beta_i)}\right)_x \left({}^{-}\phi_n^{(\beta_i')}, {}^{-}\phi_k^{(\beta_i')}\right)_t \\ &+ k_3\left({}_{-1}D_x^{\alpha}\,{}^{-}\phi_m^{(\beta_i)}, {}^{-}\phi_j^{(\beta_i)}\right)_x \left({}^{-}\phi_n^{(\beta_i')}, {}^{-}\phi_k^{(\beta_i')}\right)_t\Bigg] \\ &+ \left(\mathcal{N}(u_{M,N},\cdot), {}^{-}\phi_j^{(\beta_i)}\,{}^{-}\phi_k^{(\beta_i')}\right) = 0.\end{aligned}$$

Define the $(M{+}1)\times(M{+}1)$ x-matrices and $(N{+}1)\times(N{+}1)$ t-matrices as follows:

$$\mathbf{G}_x = \left(({}^{-}\phi_m^{(\beta_i)}, {}^{-}\phi_j^{(\beta_i)})_x\right)_{j,m}, \quad \mathbf{D}_x = \left((\partial_x\,{}^{-}\phi_m^{(\beta_i)}, {}^{-}\phi_j^{(\beta_i)})_x\right)_{j,m}, \quad \mathbf{F}_x^{(\alpha)} = \left(({}_{-1}D_x^{\alpha}\,{}^{-}\phi_m^{(\beta_i)}, {}^{-}\phi_j^{(\beta_i)})_x\right)_{j,m},$$

$$\mathbf{G}_t = \left(({}^{-}\phi_n^{(\beta_i')}, {}^{-}\phi_k^{(\beta_i')})_t\right)_{k,n}, \quad \mathbf{T}_t = \left((\partial_t\,{}^{-}\phi_n^{(\beta_i')}, {}^{-}\phi_k^{(\beta_i')})_t\right)_{k,n}, \quad \mathbf{C}_t^{(\gamma)} = \left(({}_{-1}^{C}D_t^{\gamma}\,{}^{-}\phi_n^{(\beta_i')}, {}^{-}\phi_k^{(\beta_i')})_t\right)_{k,n}.$$

Using the notation $\mathbf{u} := \mathrm{vec}(\mathcal{U}) \in \mathbb{R}^{(M+1)(N+1)}$ and the fact that

$$\mathrm{vec}(AUB^T) = (B \otimes A)\,\mathrm{vec}(U),$$

the linear part of (4.2) can be written in a compact form as

$$\mathbf{A}_{\mathrm{lin}} = \mathbf{G}_x \otimes \mathbf{C}_t^{(\gamma)} + k_1\,\mathbf{G}_x \otimes \mathbf{T}_t + k_2\,\mathbf{D}_x \otimes \mathbf{G}_t + k_3\,\mathbf{F}_x^{(\alpha)} \otimes \mathbf{G}_t.$$

The nonlinear residual is formulated as

$$r(\mathbf{u}) := A_{\mathrm{lin}}\mathbf{u} + \mathbf{n}(\mathbf{u}) = 0,$$

where the nonlinear contribution is given by

$$[\mathbf{n}(\mathbf{u})]_{(j,k)} := \langle \mathcal{N}(\Psi_x \mathcal{U} \Psi_t^T, t), -\phi_j^{(\beta_i)}\phi_k^{(\beta_i')}\rangle.$$

In the special case of a linear model, where $\mathcal{N}(u,t) = k_4 u - f(x,t)$, the load matrix $\mathbf{F}$ is introduced through quadrature as

$$(\mathbf{F})_{j,k} = \int_{-1}^{1}\int_{-1}^{1} f(x,t)\,\phi_j^{(\beta_i)}(x)\,\phi_k^{(\beta_i')}(t)\,dx\,dt.$$

We also define the mass matrix by

$$\mathbf{M} := G_x \otimes G_t.$$

The linear system then becomes

$$\Big(\mathbf{A}_{\text{lin}} + k_4\,\mathbf{M}\Big)\mathbf{u} = \text{vec}(\mathbf{F}).$$

The Kronecker form enables Sylvester-type solvers or preconditioned Krylov methods with matrix–free matvecs.

The nonlinear residual equation $\mathbf{r}(\mathbf{u}) = 0$ has been derived and discussed. To solve such a nonlinear equation, several numerical methods can be employed, including Newton's method. At each iteration, the new solution is obtained as:

$$\mathbf{u}_{k+1} = \mathbf{u}_k - \mathbf{J}^{-1}(\mathbf{u}_k)\mathbf{r}(\mathbf{u}_k),$$

where $\mathbf{J}(\mathbf{u}_k)$ denotes the Jacobian matrix associated with the derivative of the residual function $\mathbf{r}(\mathbf{u})$ relative to $\mathbf{u}$.

Combined with Newton's method, alternative iterative techniques such as relaxation approaches, quasi-Newton schemes, and other higher-order techniques may also be employed, depending on the available computational resources and the nature of the problem.

Alternatives are especially beneficial when improved accuracy is required or when exact derivatives are costly to evaluate. The selected solution procedure is influenced by the computational budget and the structure of the nonlinear residual. While several approaches exist, Newton's method is often a reliable choice for solving the present formulation, preferred due to its rapid convergence for well-posed nonlinear problems

5. Numerical Examples

In this section, we provide a set of numerical tests to illustrate the performance of the proposed Hybrid Müntz–Jacobi Spectral Galerkin approach when applied to space–time fractional advection–diffusion equations. To facilitate the computations, the problem is reformulated on the normalized interval $[-1, 1]$ by means of an affine transformation.

Example 5.1. *Consider the following time–fractional advection–diffusion equation for* $0 < \alpha < 1$ *[30]:*

$${}^{C}_{-1}D^{\gamma}_{t}u(x,t) + \frac{\partial^2}{\partial x^2}u(x,t) + u(x,t) = f(x,t), \quad x \in (-1,1), \quad t \in (0,1],$$

with the boundary and initial conditions $u(\pm 1, t) = u(x, 0) = 0$.

The corresponding exact solution is given by

$$u(x,t) = \sin(\pi x)\sin(\pi t^{\alpha}).$$

This example is solved using the Hybrid Müntz–Jacobi Spectral Galerkin Method proposed in this work. For the numerical experiments, we set $N = M = 20$. The parameters of the method are chosen as

$$(\beta_i) = (\varepsilon, 1-\varepsilon, 1),$$

where ε is a sufficiently small positive number. For $\alpha = 0.2$, the parameters are selected as $(\beta_i') = (0.2, 0.4, 0.6)$, and for $\alpha = 0.9$, we use $(\beta_i') = (0.7, 0.8, 0.9)$. The corresponding numerical solutions are illustrated in Figures 1–2. Furthermore, the maximum absolute error for $N = M = 20$ is reported in Figures 3–4. The numerical experiments demonstrate rapid convergence of the method towards the exact solution.

Specifically, the accuracy improves as the parameter α increases, and the scheme can cope effectively with the challenges posed by space-time fractional models.

The results also demonstrate that the approach achieves both efficiency and accuracy . As displayed in Figures 1–4, the error analysis confirms that the method converges reliably for a wide range of values of α. This indicates the robustness of the proposed method in handling time-dependent problems and fractional derivatives.

Figures 3– ref fig4 show the absolute error for the case $N = M = 20$, providing insight into the error distribution for different values of α. The data reveal that the error decreases as N and M grow, illustrating that the method attains high accuracy even when the number of basis functions is relatively modest.

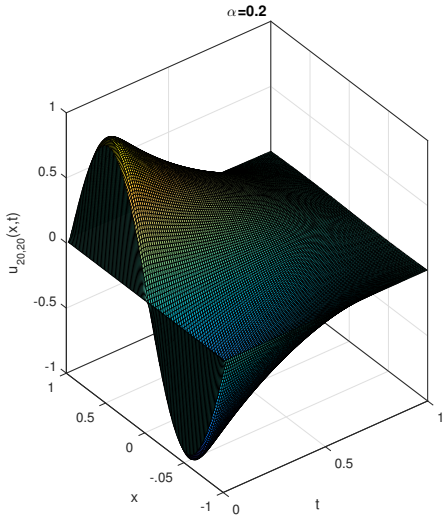

FIGURE 1. Surface plots of $u_{20,20}(x,t)$ for $\alpha = 0.2$.

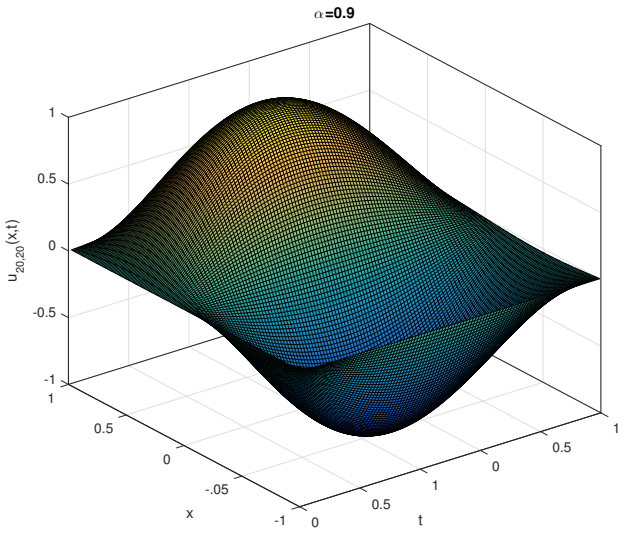

FIGURE 2. Surface plots of $u_{20,20}(x,t)$ for $\alpha = 0.2$.

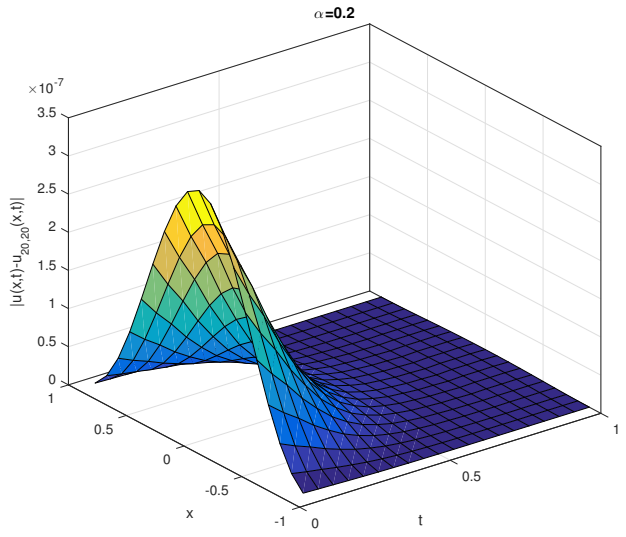

FIGURE 3. The values of $|u_{20,20}(x,t) - u(x,t)|$ errors for $\alpha = 0.2$.

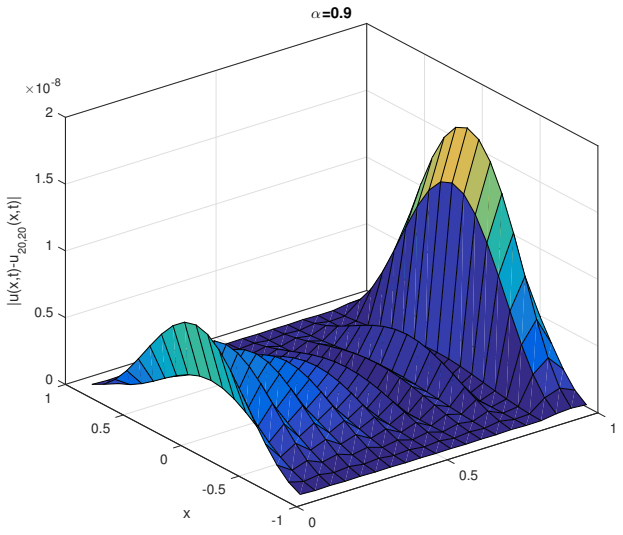

FIGURE 4. The values of $|u_{20,20}(x,t) - u(x,t)|$ errors for $\alpha = 0.2$.

Example 5.2. *Consider the following time- and space-fractional advection–diffusion problem:*

$$ {}_0^C D_t^{\gamma} u(x,t) + {}_0 D_x^{\alpha_1} u(x,t) + {}_0 D_x^{1+\alpha_2} u(x,t) = f(x,t), \quad x \in [-1,1],\ t \in (0,1], \tag{5.1} $$

subject to the homogeneous boundary and initial conditions

$$ u(\pm 1, t) = u(x,0) = 0. $$

The exact solution of the problem is expressed as

$$ u_{\text{exact}}(x,t) = t^{6+\frac{2}{3}} \left[(1+x)^{6+\frac{9}{17}} - 2(1+x)^{5+\frac{9}{17}} \right]. \tag{5.2} $$

This equation has been studied in [39], a fractional spectral collocation method was proposed by Zayernouri and Karniadakis. Using this approach, the authors derived fractional differentiation matrices and demonstrated that the method yields exponential convergence when applied to time- and space-fractional advection-diffusion problems.

Building on the work of [39], we solve this example for different values of (α_1, α_2) and γ. The numerical solution is obtained using the present method, and the accuracy is calculated using the maximum (infinity norm) error at $t = 0.5$ for different values of $N(= M)$, which denotes the number of basis functions in both spatial and temporal directions.

The results, illustrated in Figure 5, clearly demonstrate the efficiency of the method: the errors decrease rapidly as N increases, confirming the good performance of the present approach in line with the exponential convergence reported in [39].

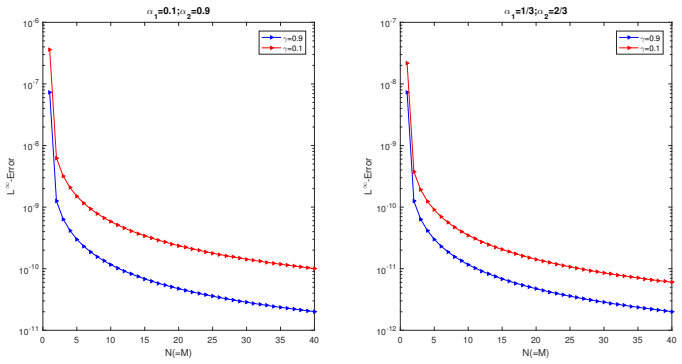

FIGURE 5. The L^{∞}-errors for various values of α and γ at $t = 0.5$.

Example 5.3. *We consider the following nonlinear time-fractional advection–diffusion equation defined on* $t \in [0,1]$ *and* $x \in [0,\pi]$*:*

$$ {}_0^C D_t^{\alpha} u(x,t) - \Delta u(x,t) + u(x,t) + u^2(x,t) = f(x,t), $$

with homogeneous boundary and initial conditions

$$ u(0,t) = u(\pi,t) = 0, \qquad u(x,0) = \sin(x), $$

and the forcing term

$$ f(x,t) = \sin(x)\Big(\Gamma(\alpha+2)t + (\alpha+1)t^{\alpha} + 2(t^{\alpha+1}+1)\Big) + (t^{\alpha+1}+1)^2 \sin^2(x). $$

The analytical solution for this problem is expressed as

$$ u(x,t) = (t^{\alpha+1}+1)\sin(x). $$

This problem has been studied in two previous works: in [8] using the Uniform Cubic B-Spline Method (UCBSM) with $m = 100$ basis functions, and in [3] where generalized Bernstein-like basis functions (GBFs) were used within a space-time Galerkin framework.

In the present work, the problem is addressed through a Hybrid Müntz–Jacobi Spectral Galerkin Method with parameters

$$ \beta = (\varepsilon, 1-\varepsilon, 1), \qquad \beta' = (\alpha, \beta_2, \beta_3), $$

and truncation numbers $M = N = 8$. For a fair comparison, all methods are tested at $t = 0.1$, and the absolute errors are reported for different x values.

The results of our method with $M = N = 8$ compared with those of [8] with $m = 100$ and [3] with $M = N = 12$ are summarized in Table 1. It is evident that the present method yields significantly smaller errors than both UCBSM and GBF-based spectral methods.

TABLE 1. Absolute error values achieved using the proposed method, UCBSM [8], and GBF-based spectral method [3] for $t = 0.1$.

x	UCBSM [8]		GBFs [3]		Present method	
x	$\alpha = 1.5$	$\alpha = 1.9$	$\alpha = 1.5$	$\alpha = 1.9$	$\alpha = 1.5$	$\alpha = 1.9$
0.31415	1.01e-04	8.83e-05	1.29e-11	4.91e-12	1.12e-14	2.58e-14
0.942478	2.67e-04	2.31e-04	3.93e-11	2.17e-11	5.26e-14	1.89e-15
1.5708	3.33e-04	2.87e-04	3.34e-11	1.05e-10	9.19e-14	3.95e-14
2.19911	2.67e-04	2.31e-04	3.60e-11	3.41e-11	2.78e-15	8.12e-15
2.82743	1.01e-04	8.83e-05	2.92e-11	5.61e-11	6.03e-15	7.29e-15

Furthermore, in Figure 6, the error values $|u(x,t) - u_{8,8}(x,t)|$ for different values of α are displayed using the present method. Additionally, Figure 7 shows the error distribution $|u(x,t) - u_{8,8}(x,t)|$ for $\alpha = 0.2$ with respect to different t values for various x. These figures confirm the superior accuracy and robustness of the proposed Hybrid Müntz–Jacobi Spectral Galerkin Method.

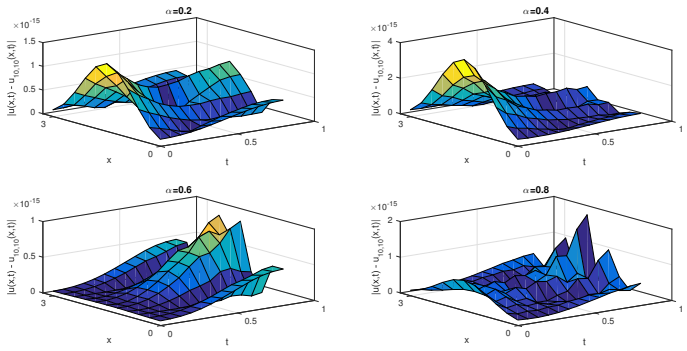

FIGURE 6. The error values $|u(x,t) - u_{8,8}(x,t)|$ for different values of α.

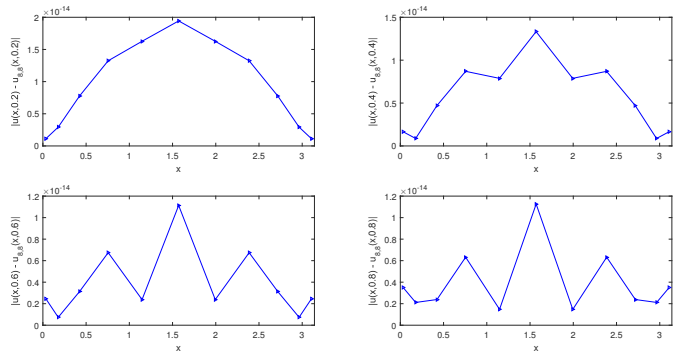

FIGURE 7. The error distribution $|u(x,t) - u_{8,8}(x,t)|$ for $\alpha = 0.2$ with respect to different t values for various x.

TABLE 2. Evaluation of L^2 errors obtained using the proposed method in comparison with the method of [27], across several values of α.

	Method in [27]			present Method			
M, N	$\alpha = 0.2$	$\alpha = 0.4$	$\alpha = 0.6$	M, N	$\alpha = 0.2$	$\alpha = 0.4$	$\alpha = 0.6$
32	1.37e-1	6.25e-3	6.75e-4	5	12.25e-7	1.51e-8	1.17e-9
64	7.57e-2	1.64e-3	1.75e-4	10	1.89e-8	6.25e-8	6.28e-10
128	4.00e-2	4.26e-4	4.65e-5	15	4.59e-9	4.29e-9	1.87e-10
256	2.07e-2	1.09e-4	1.23e-5	20	8.20e-10	2.41e-10	2.08e-11

Example 5.4. *Consider the following time-fractional diffusion equation:*

$$ {}_0^C D_t^\alpha u(x,t) - \frac{\partial^2 u(x,t)}{\partial x^2} = f(x,t), \qquad (x,t) \in (0,\pi) \times (0,1], $$

subject to the initial and boundary conditions

$$ u(0,t) = u(\pi,t) = 0, \quad t \in (0,1], \qquad u(x,0) = e^{\frac{x}{2}} \sin(x), \quad x \in [0,\pi]. $$

The source term $f(x,t)$ is chosen such that the exact solution is given by

$$ u(x,t) = E_{\alpha,1}(-1.25\, t^\alpha)\, e^{\frac{x}{2}} \sin(x), $$

where $E_{\alpha,\beta}(z)$ denotes the two-parameter Mittag–Leffler function

$$ E_{\alpha,\beta}(z) = \sum_{k=0}^{\infty} \frac{z^k}{\Gamma(\alpha k + \beta)}, \qquad \alpha, \beta > 0. $$

This problem was previously studied in [27], where a finite-difference type scheme was introduced. In that approach, the Caputo time-fractional derivative was approximated through the L2–1σ discretization, while the spatial second-order derivative was handled using the standard central difference technique on uniform meshes.

In this study, we address the same problem by employing a Hybrid Müntz–Jacobi Spectral Galerkin Method. In contrast to finite-difference formulations, the proposed strategy utilizes specially designed hybrid basis functions that combine Jacobi and Müntz-type components, enabling an efficient representation of the singular features of fractional-order solutions. This framework leads to highly accurate numerical approximations while involving substantially fewer basis functions.

Furthermore, Figure 8 shows the numerical results corresponding to several choices of α, which verify the robustness of the method in terms of efficiency and stability.

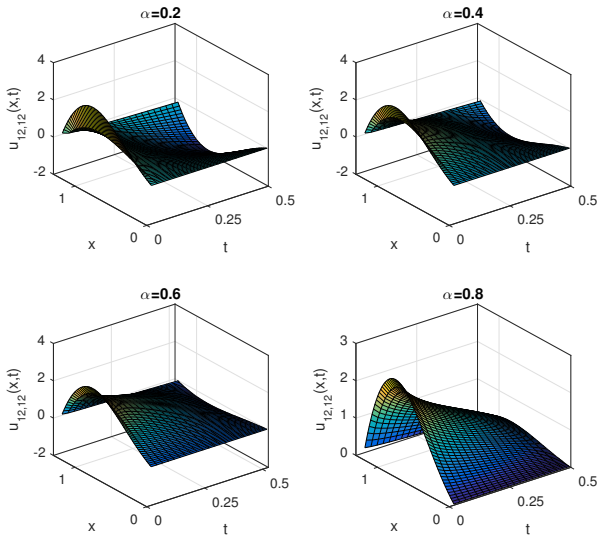

FIGURE 8. Approximate solutions for different values of α produced by the proposed method.

6. Discussion

In this work, the hybrid Müntz-Jacobi Galerkin method is used to solve the space-time fractional advection-diffusion equation numerically, which yields highly accurate results.

Due to the inherent property of the hybrid bases, which are constructed based on the singular indices of the unknown solutions, it is relatively superior to methods that use classical polynomials to solve fractional equations. Hence, it results in high convergence rates in many problems with non-smooth solutions.

This advantage is clearly shown in Tables 1 and 2. The singular form of Müntz bases is combined with Jacobi polynomials and can be used for fractional problems in general with high flexibility.

For future research, this method can be applied to more complex fractional problems or systems of fractional equations that can have a range of irregular domains

7. Conclusion

We present a spectral Galerkin approach to solve the space-time fractional advection-diffusion equation numerically. Due to the singular nature of the kernel in the definition of fractional operators, most fractional problems have non-smooth solutions. Then, we defined the approximation space of the basis functions as a combination of Müntez-Jacobi functions. In these bases, the singular form of the bases is stably combined with Jacobian polynomials. To adapt to the physical constraints of the problem and keep the discrete algebraic system stable, we have adjusted them to homogeneous conditions. These defined bases have the potential to handle nonlinear problems and coupled systems of equations. This framework can be developed both practically and theoretically for fractional PDEs. Overall, the proposed approach brings some beneficial properties: the

flexibility of Müntz systems for handling singularities and the orthogonality of Jacobi polynomials, which makes the discretization stable and well-posed.

Conflicts of Interest: The authors declare that there are no conflicts of interest regarding the publication of this paper.

References

[1] M. Dehghan, M. Abbaszadeh, W. Deng, Fourth-Order Numerical Method for the Space–Time Tempered Fractional Diffusion-Wave Equation, Appl. Math. Lett. 73 (2017), 120–127. https://doi.org/10.1016/j.aml.2017.04.011.

[2] M. Abbaszadeh, M. Dehghan, A Finite-Difference Procedure to Solve Weakly Singular Integro Partial Differential Equation with Space-Time Fractional Derivatives, Eng. Comput. 37 (2021), 2173–2182. https://doi.org/10.1007/s00366-020-00936-w.

[3] A.T. Algazaa, J. Saeidian, Spectral Methods Utilizing Generalized Bernstein-like Basis Functions for Time-Fractional Advection-Diffusion Equations, Math. Methods Appl. Sci. 48 (2025), 1411–1429. https://doi.org/10.1002/mma.10390.

[4] M.H. Alshbool, O. Isik, I. Hashim, Fractional Bernstein Series Solution of Fractional Diffusion Equations with Error Estimate, Axioms 10 (2021), 6. https://doi.org/10.3390/axioms10010006.

[5] M. Almushaira, F. Chen, F. Liu, Efficient Operator Splitting and Spectral Methods for the Time-Space Fractional Black–Scholes Equation, Results Appl. Math. 10 (2021), 100149. https://doi.org/10.1016/j.rinam.2021.100149.

[6] M. Almushaira, H. Bhatt, A.M. Al-rassas, Fast High-Order Method for Multi-Dimensional Space-Fractional Reaction–Diffusion Equations with General Boundary Conditions, Math. Comput. Simul. 182 (2021), 235–258. https://doi.org/10.1016/j.matcom.2020.11.001.

[7] G.A. Anastassiou, Advances on Fractional Inequalities, Springer New York, 2011. https://doi.org/10.1007/978-1-4614-0703-4.

[8] O. Abu Arqub, S. Tayebi, D. Baleanu, M.S. Osman, W. Mahmoud, H. Alsulami, A Numerical Combined Algorithm in Cubic B-Spline Method and Finite Difference Technique for the Time-Fractional Nonlinear Diffusion Wave Equation with Reaction and Damping Terms, Results Phys. 41 (2022), 105912. https://doi.org/10.1016/j.rinp.2022.105912.

[9] A. Babaaghaie, K. Maleknejad, A New Approach for Numerical Solution of Two-Dimensional Nonlinear Fredholm Integral Equations in the Most General Kind of Kernel, Based on Bernstein Polynomials and Its Convergence Analysis, J. Comput. Appl. Math. 344 (2018), 482–494. https://doi.org/10.1016/j.cam.2018.06.002.

[10] P. Borwein, T. Erdélyi, Polynomials and Polynomial Inequalities, Springer New York, 1995. https://doi.org/10.1007/978-1-4612-0793-1.

[11] S. Chen, J. Shen, L.L. Wang, Generalized Jacobi Functions and Their Applications to Fractional Differential Equations, Math. Comput. 85 (2016), 1603–1638. https://doi.org/10.1090/mcom3035.

[12] K. Diethelm, The Analysis of Fractional Differential Equations, Springer Berlin Heidelberg, 2010. https://doi.org/10.1007/978-3-642-14574-2.

[13] E.H. Doha, W.M. Abd-Elhameed, Y.H. Youssri, Fully Legendre Spectral Galerkin Algorithm for Solving Linear One-Dimensional Telegraph Type Equation, Int. J. Comput. Methods 16 (2019), 1850118. https://doi.org/10.1142/s0219876218501189.

[14] S. Erfani, E. Babolian, S. Javadi, New Fractional Pseudospectral Methods with Accurate Convergence Rates for Fractional Differential Equations, Electron. Trans. Numer. Anal. 54 (2021), 150–175. https://doi.org/10.1553/etna_vol54s150.

[15] J. Eshaghi, S. Kazem, H. Adibi, The Local Discontinuous Galerkin Method for 2D Nonlinear Time-Fractional Advection–Diffusion Equations, Eng. Comput. 35 (2019), 1317–1332. https://doi.org/10.1007/s00366-018-0665-8.

[16] R. Gorenflo, S. Vessella, Abel Integral Equations, Springer Berlin Heidelberg, 1991. https://doi.org/10.1007/bfb0084665.

[17] A.A. Kilbas, H.M. Srivastava, J.J. Trujillo, Theory and Applications of Fractional Differential Equations, North-Holland Mathematics Studies, vol. 204, Elsevier, Amsterdam, 2006. https://shop.elsevier.com/books/theory-and-applications-of-fractional-differential-equations/kilbas/978-0-444-51832-3.

[18] C. Li, F. Zeng, F. Liu, Spectral Approximations to the Fractional Integral and Derivative, Fract. Calc. Appl. Anal. 15 (2012), 383–406. https://doi.org/10.2478/s13540-012-0028-x.

[19] Z. Li, Z. Liang, Y. Yan, High-Order Numerical Methods for Solving Time Fractional Partial Differential Equations, J. Sci. Comput. 71 (2016), 785–803. https://doi.org/10.1007/s10915-016-0319-1.

[20] G.V. Milovanović, Müntz Orthogonal Polynomials and Their Numerical Evaluation, in: W. Gautschi, G. Opfer, G.H. Golub, (eds) Applications and Computation of Orthogonal Polynomials, Birkhäuser Basel, pp. 179–194, (1999). https://doi.org/10.1007/978-3-0348-8685-7_13.

[21] F. Mainardi, Fractional Calculus and Waves in Linear Viscoelasticity, World Scientific, 2013. https://doi.org/10.1142/p926.

[22] F. Mirzaee, N. Samadyar, Combination of Finite Difference Method and Meshless Method Based on Radial Basis Functions to Solve Fractional Stochastic Advection–Diffusion Equations, Eng. Comput. 36 (2019), 1673–1686. https://doi.org/10.1007/s00366-019-00789-y.

[23] M. Ghasemi, K. Mohammadi, A. Alipanah, Numerical Solution of System of Second-Order Integro-Differential Equations Using Nonclassical Sinc Collocation Method, Bound. Value Probl. 2023 (2023), 38. https://doi.org/10.1186/s13661-023-01724-3.

[24] P. Borwein, T. Erdélyi, J. Zhang, Müntz Systems and Orthogonal Müntz-Legendre Polynomials, Trans. Am. Math. Soc. 342 (1994), 523–542. https://doi.org/10.1090/S0002-9947-1994-1227091-4.

[25] I. Podlubny, Fractional Differential Equations, Academic Press, 1999.

[26] M. Almushaira, A Linearized Spectral Collocation Method for Riesz Space Fractional Nonlinear Reaction–Diffusion Equations, Comput. Math. Methods 3 (2021), ahead of print. https://doi.org/10.1002/cmm4.1177.

[27] H. Qiao, A. Cheng, Finite Difference Method on Non-Uniform Meshes for Time Fractional Diffusion Problem, Comput. Methods Appl. Math. 21 (2020), 899–911. https://doi.org/10.1515/cmam-2020-0077.

[28] J. Rashidinia, A. Momeni, Collocation Method for Solving Fractional Reaction–Diffusion Problem Arising in Chemistry, Sci. Rep. 15 (2025), 22348. https://doi.org/10.1038/s41598-025-05339-9.

[29] L. Sadek, A.S. Bataineh, O.R. Isik, H.T. Alaoui, I. Hashim, A Numerical Approach Based on Bernstein Collocation Method: Application to Differential Lyapunov and Sylvester Matrix Equations, Math. Comput. Simul. 212 (2023), 475–488. https://doi.org/10.1016/j.matcom.2023.05.011.

[30] C. Sheng, J. Shen, A Space-Time Petrov-Galerkin Spectral Method for Time Fractional Diffusion Equation, Numer. Math. Theory Methods Appl. 11 (2018), 854–876. https://doi.org/10.4208/nmtma.2018.s10.

[31] J. Shen, T. Tang, L. Wang, Spectral Methods, Springer Berlin Heidelberg, 2011. https://doi.org/10.1007/978-3-540-71041-7.

[32] J. Shen, Y. Wang, Müntz-Galerkin Methods and Applications to Mixed Dirichlet-Neumann Boundary Value Problems, SIAM J. Sci. Comput. 38 (2016), A2357–A2381. https://doi.org/10.1137/15m1052391.

[33] L. Shi, S. Rashid, S. Sultana, A. Khalid, P. Agarwal, et al., Semi-Analytical View of Time-Fractional PDEs with Proportional Delays Pertaining to Index and Mittag-Leffler Memory Interacting with Hybrid Transforms, Fractals 31 (2023), 2340071. https://doi.org/10.1142/S0218348X23400716.

[34] S. Vong, Z. Wang, A Compact Difference Scheme for a Two Dimensional Fractional Klein–Gordon Equation with Neumann Boundary Conditions, J. Comput. Phys. 274 (2014), 268–282. https://doi.org/10.1016/j.jcp.2014.06.022.

[35] M. Yarmohammadi, S. Javadi, E. Babolian, Spectral Iterative Method and Convergence Analysis for Solving Nonlinear Fractional Differential Equation, J. Comput. Phys. 359 (2018), 436–450. https://doi.org/10.1016/j.jcp.2018.01.020.

[36] M. Yarmohammadi, S. Javadi, Piecewise Fractional Interpolation with Application to Fractional Differential Equations, J. Sci. Comput. 86 (2021), 18. https://doi.org/10.1007/s10915-020-01373-z.

[37] D. Zeidan, C.K. Chau, T.T. Lu, W.Q. Zheng, Mathematical Studies of the Solution of Burgers' Equations by Adomian Decomposition Method, Math. Methods Appl. Sci. 43 (2019), 2171–2188. https://doi.org/10.1002/mma.5982.

[38] S. Kumar, D. Zeidan, An Efficient Mittag-Leffler Kernel Approach for Time-Fractional Advection-Reaction-Diffusion Equation, Appl. Numer. Math. 170 (2021), 190–207. https://doi.org/10.1016/j.apnum.2021.07.025.

[39] M. Zayernouri, G.E. Karniadakis, Fractional Spectral Collocation Method, SIAM J. Sci. Comput. 36 (2014), A40–A62. https://doi.org/10.1137/130933216.

[40] F. Zeng, C. Li, F. Liu, I. Turner, The Use of Finite Difference/Element Approaches for Solving the Time-Fractional Subdiffusion Equation, SIAM J. Sci. Comput. 35 (2013), A2976–A3000. https://doi.org/10.1137/130910865.

[41] F. Sabzikar, M.M. Meerschaert, J. Chen, Tempered Fractional Calculus, J. Comput. Phys. 293 (2015), 14–28. https://doi.org/10.1016/j.jcp.2014.04.024.